ELSEVIER

Journal of Nuclear Materials 313–316 (2003) 743–747

journal of nuclear materials

www.elsevier.com/locate/jnucmat

Photon efficiency $(S + D)/XB$ of hydrogen molecules at low electron temperatures

U. Fantz [a,*], B. Heger [a,b], D. Wünderlich [a,b], R. Pugno [b], ASDEX Upgrade Team [b]

[a] *Lehrstuhl für Experimentelle Plasmaphysik, Universität Augsburg, D-86135 Augsburg, Germany*
[b] *Max-Planck-Insitut für Plasmaphysik, EURATOM Association, D-85748 Garching, Germany*

Abstract

The determination of molecular hydrogen fluxes in the plasma edge of fusion experiments from molecular radiation requires the precise knowledge of photon efficiencies $(S + D)/XB$, i.e. the ionization and dissociation processes per emitted photon. Photon efficiencies are calculated by a collisional radiative model for molecular hydrogen which gives dependencies on electron temperature, on electron density and on the vibrational population of the molecule in its ground state. To prove the model, photon efficiencies are measured by gas puffing experiments in the divertor of ASDEX Upgrade at high electron densities ($n_e \approx 10^{19}$ m^{-3}) and low electron temperatures ($T_e \approx 10$ eV). Furthermore, results from laboratory plasmas ($n_e \approx 10^{17}$ m^{-3}, $T_e \approx 3$ eV) are also used for an experimental check of the model. The comparison allows an identification of relevant processes such as dissociative attachment from excited states of hydrogen, thus improving molecular hydrogen diagnostics.

PACS: 52.40.Hf; 52.70.Nc; 52.25.Rv
Keywords: Plasma-wall interaction; Divertor; Boundary plasmas; Hydrogen molecules; Collisional radiative model; Spectroscopy

1. Introduction

In fusion experiments plasma recycling takes place in the scrape-off layer [1]. In attached plasmas, the particles recombine at the solid surfaces and are released into the plasma where they undergo a variety of reactions, e.g. ionization or charge exchange. At the surfaces the particles can recombine either to hydrogen atoms or hydrogen molecules. As shown in [2], the ratio of these species depends on the temperature of the surface. Additionally, impurities are produced as well, e.g. methane by chemical erosion of carbon which is often used as wall material. In fusion devices with divertor, the divertor can operate in various recycling regimes, i.e. low recycling, high recycling and detachment. In the latter case, electron temperatures are low and the molecular hydrogen fluxes are comparable to atomic fluxes [3]. All mentioned species affect the plasma edge and have to be considered in plasma edge codes. In case of hydrogen, the reaction chain is more complex for molecules than for atoms. Molecular hydrogen has metastable vibrational levels in the ground state, which open very effective new reaction channels such as dissociative attachment $(H_2(v) + e \rightarrow H^- + H)$ and ion conversion $(H_2(v) + H^+ \rightarrow H_2^+ + H)$ and can influence the energy balance of the plasma [3]. Therefore, it is very important to know the quantity of molecules released from the surface in a wide parameter range.

Particle fluxes are frequently deduced by emission spectroscopy in the visible spectral range [4]. The correlation of measured photon fluxes with particle influxes

* Corresponding author. Address: Lehrstuhl für Experimentelle Plasmaphysik, Universität Augsburg, Universitätsstrasse, D-86135 Augsburg, Germany. Tel.: +49-821 598 3310; fax: +49-821 598 3302.
E-mail address: fantz@physik.uni-augsburg.de (U. Fantz).

0022-3115/03/$ - see front matter © 2003 Elsevier Science B.V. All rights reserved.
PII: S0022-3115(02)01492-7

is given by the so-called photon efficiency. For example, impurity influxes of methane are correlated with the radiation emitted from the CH band (around 431 nm) by the photon efficiency D/XB which describes the dissociation events per emitted photon. This ratio is calculated from the molecular break-up of methane. Atomic hydrogen influxes can be determined from the H_α radiation and the photon efficiency S/XB, i.e. the number of ionization per emitted H_α Balmer photon, which is calculated by collisional radiative models for hydrogen atoms [5,6]. Balmer radiation is also emitted due to dissociative excitation of hydrogen molecules or dissociation of molecular ions. In case of high molecular influxes these processes have to be considered also in the calculation of photon efficiencies for atoms.

In case of molecular hydrogen, the Fulcher band (electronic transition: $d^3\Pi_u - a^3\Sigma_g^+$, vibrational bands: $v' = v'' = 0$–3, wavelength range: 600–640 nm) is commonly used to measure molecular hydrogen influxes [2,3]. The calculation of the photon efficiency $(S+D)/\mathrm{XB}$, i.e. ionization and dissociation processes per emitted Fulcher photon, is based on the collisional radiative model of Sawada [7]. Since the photon efficiency varies with plasma parameters up to three orders of magnitude the underlying collisional radiative model has to be proved by experimental investigations, which is the aim of this paper.

2. Photon efficiency $(S+D)/\mathrm{XB}$

The photon efficiency $(S+D)/\mathrm{XB}$ relates the measured photon flux $\Gamma_{\mathrm{photons}}$ to the molecular hydrogen influx Γ_{H_2} released from the plasma facing materials:

$$\Gamma_{H_2} = \frac{(S+D)}{\mathrm{XB}} \Gamma_{\mathrm{photons}}. \quad (1)$$

S is the effective ionization rate coefficient, D is the effective dissociation rate coefficient and XB denotes the effective emission rate coefficient for the Fulcher radiation. All three rate coefficients depend, in general, on the plasma parameters electron temperature T_e and electron density n_e and are calculated by a collisional radiative model (see Section 2.1). Using an absolutely calibrated spectroscopic system, the intensities of the rotational lines of the various vibrational bands of the Fulcher transition give a rotational temperature, a vibrational population in the excited state and finally the whole Fulcher photon flux $\Gamma_{\mathrm{photons}}$ [3]. If the molecular hydrogen flux is known, the photon efficiency can be determined from the measured Fulcher photon flux. This can be achieved by gas puffing experiments (see Section 2.2.) with calibrated flow meters. For a comparison of measured photon efficiencies with calculated ones, the plasma parameters must be well-known. In a next step, the calculations are discussed on the basis of the input data.

2.1. Calculations

The calculation of photon efficiencies is based on a collisional radiative model for H_2 [8], which is an extension of the collisional radiative model by Sawada [7]. Besides the electronic states the vibrational levels in the ground state of the molecule are taken into account. The electronic states in the principal quantum number $n = 2$ are resolved whereas all other excited states are only separated with respect to the multiplet system. The upper state of the Fulcher transition ($d^3\Pi_u$) is one of the six $n = 3$ states (unresolved) in the triplet system. According to the small maximum energy difference of 0.8 eV, the relative population among these levels are assumed to be given by the statistical weights. The effective emission rate coefficient for the Fulcher band XB is then deduced from the population density of $n = 3$, n_3:

$$\mathrm{XB}(d^3\Pi_u - a^3\Sigma_g^+) = n_3 \times 2/7 \times A_{\mathrm{Fulcher}}/(n_e \times n_{H_2}). \quad (2)$$

2/7 is the ratio of the statistical weight of the $d^3\Pi_u$ state to the sum of all six states, A_{Fulcher} is the Einstein transition probability for the Fulcher emission ($A_{\mathrm{Fulcher}} = 2.5 \times 10^7\ \mathrm{s}^{-1}$ [9]) and n_{H_2} denotes the molecular hydrogen density.

The main reactions which contribute to the effective ionization rate coefficient S are (i) electron impact ionization from the ground state, (ii) electron impact ionization from electronically excited states and (iii) ion conversion (vibrationally resolved), which is dominant in the low energy range. The effective dissociation rate coefficient is determined by (i) electron impact excitation of the repulsive state $b^3\Sigma_u^+$ from the ground state (vibrationally resolved), (ii) electron impact excitation of electronic states in the triplet system followed by de-excitation into $b^3\Sigma_u^+$ and (iii) dissociative excitation into excited atomic hydrogen followed by radiative decay. The calculation of the vibrational population is implemented in the collisional radiative model [8]. Thus, the photon efficiency depends on T_e, on n_e and on the vibrational population in the ground state as shown in Fig. 1. The dependence on vibrational population is illustrated only for $n_e = 10^{20}\ \mathrm{m}^{-3}$.

In contrast to the effective ionization and dissociation rate coefficients, the effective emission rate coefficient of the Fulcher radiation is uncertain. The dominant population mechanism of the $n = 3$ state in the triplet system is electron impact excitation from the ground state and from the metastable state $c^3\Pi_u$ ($n = 2$) [3]. Therefore, the question arises whether the $c^3\Pi_u$ level will remain metastable or will be de-excited by collisional quenching and which input data base should be used for direct electron impact excitation. As discussed in [10], the various excitation rate coefficients given in literature differ by a factor of seven, which results in an uncertainty in the effective emission rate coefficient of a factor

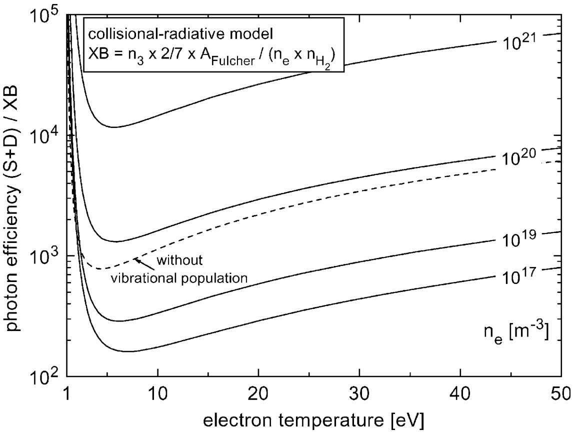

Fig. 1. Calculated photon efficiency for the Fulcher radiation of hydrogen molecules on the basis of the collisional radiative model described in [8].

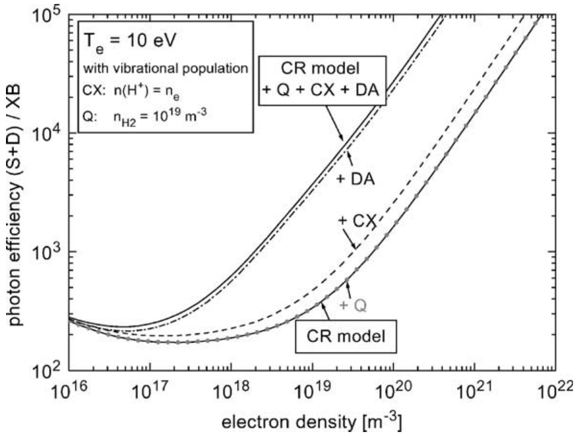

Fig. 2. Calculated photon efficiency as a function of electron density with and without extensions of the collisional radiative model (CR model, [8]): quenching (Q), charge exchange (CX) and dissociative attachment from excited states (DA).

of 1.8. Measurements of Fulcher radiation in microwave discharges at $n_e = 7 \times 10^{16}$–5×10^{17} m^{-3} and $T_e = 2$–3 eV show systematically lower radiation (factor five to ten) then predicted by the collisional radiative model for these parameters [10]. The collisional radiative model was therefore extended by three new reactions: (i) collisional de-activating process (quenching) of $n = 2$, (ii) charge exchange of excited states ($n \geqslant 2$) and (iii) dissociative attachment from excited states ($n \geqslant 2$). The rate coefficients are taken from [11] for reaction (i), from [12] for reaction (ii), from [13] ($n = 2$) and [14] ($n > 2$) for reaction (iii). Quenching is important in laboratory plasmas since molecular hydrogen is the dominant particle density. Thus, quenching processes reduce the predicted radiation by a factor of about two, which is mainly due to the depopulation of one to two orders of magnitude of the metastable state $c^3\Pi_u$. Charge exchange plays a minor role in these laboratory plasmas, whereas dissociative attachment of excited states, and in particular of the $n = 3$ states, becomes important in the investigated electron density range. The three processes together reduce the predicted radiation, so that calculations and measurements finally match by a factor of two. However, at higher electron densities dissociative attachment and charge exchange are more pronounced, whereas quenching is negligible as shown in Fig. 2 for $T_e = 10$ eV. Thus, the extended collisional radiative model has to be confirmed also at higher electron densities and low electron temperatures and the corresponding experimental campaign will be described next.

2.2. Measurements

In order to measure photon efficiencies of molecular hydrogen, gas puff experiments were carried out in hydrogen discharges of ASDEX Upgrade. Time traces of neutral beam injection (NBI) power, measured averaged electron density in the midplane (interferometry) and neutral gas density in the divertor are shown in Fig. 3. The two hydrogen L-mode discharges are nearly identical. Time intervals for gas puffing through calibrated divertor valves were set to be 0.5 s, one in the low and one in the high electron density ($\bar{n}_e$) plateau. As indicated in Fig. 3, two valves have been used, namely the upper and the lower valve in the outer divertor (divertor IIb). During the discharges the strike-point is located slightly above the lower valve (s-co-ordinate: 1.132 m), whereas the upper valve is 11.8 cm higher (s-co-ordinate: 1.250 m). The typical total particle number per gas puff was 10^{19} which has not disturbed the overall plasma performance. This has been checked by analysing a choice of standard signals, e.g. totally radiated power (P_{rad}) and plasma energy (W_{MHD}). Moreover, the H_α signal ensures that ELMs do not occur, which simplifies the analysis.

Two shots are necessary to match the spectral wavelength range of the Fulcher radiation with a 1m spectrometer and an ICCD camera, covering 14 nm per shot. Various lines of sight of the divertor spectroscopic system were used to detect the molecular radiation: VOU and VOL are widely open cones which observe the upper and lower valve, respectively. Lines of sight denoted with ROV image the plasma by lenses, ROV008 neighbouring VOL001 and ROV019 neighbouring VOU001. These two lines of sight are used to check whether the size of the gas puff in the plasma exceeds the solid angle of the volume observed by VOU or VOL. The time traces of the measured molecular hydrogen intensity (VOL001 and ROV008) are shown in the lower part of Fig. 3. The exposure time of the ICCD camera was set to 100 ms. Before the first gas puff takes place,

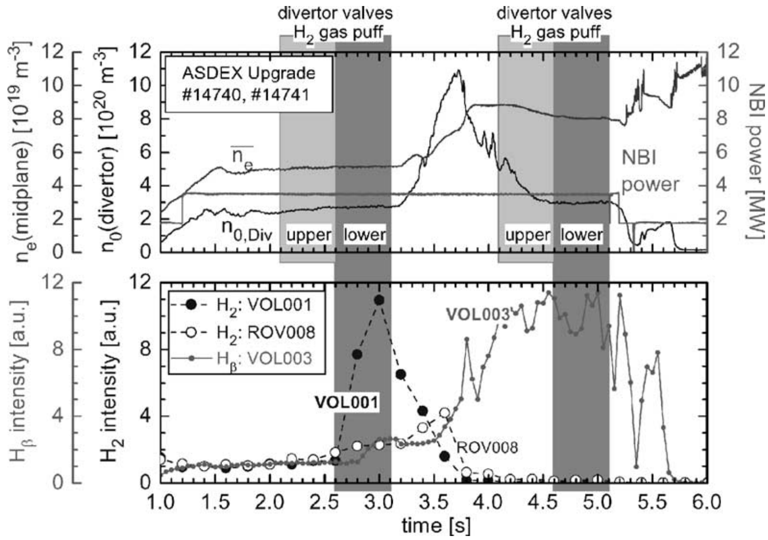

Fig. 3. Parameters of ASDEX Upgrade discharges (#14740, #14741): midplane electron density, NBI power, neutral density in the divertor together with time intervals of gas puffing in the outer divertor (lower and upper valve) as well as time traces of molecular band intensity and H_β line observed with three line of sights.

the molecular intensity (VOL001) is weak, increases during the puff and shows a decay afterwards. ROV008 remains undisturbed by the gas puff. Concerning the upper valve, the signal from ROV019 (not shown in Fig. 3) increases simultaneously with an increase of VOU001, which means that the hydrogen puff exceeds the volume observed by VOU001. Since the determination of photon efficiencies requires the observation of all particles this line of sight cannot be used for the analysis. It is remarkable that the H_β signal (VOL003) increases during the gas puff in the lower valve (Fig. 3). This increase is related to the dissociative excitation mechanism of hydrogen molecules into excited atomic hydrogen. After the first gas puff, the molecular intensity decreases and vanishes at 3.8 s, whereas the H_β line increases. The second gas puff (4.6–5.1 s) is mirrored neither in the molecular intensity nor in the Balmer line. This might be explained by the increase in n_e and T_e which strongly enhances the $(S+D)/\mathrm{XB}$ ratio such that the molecular radiation is below the detection limit and the ionization dominates over the dissociation.

3. Results and conclusions

The averaged molecular photon flux during the first gas puff in the lower divertor valve is determined to be $\Gamma_{\mathrm{photons}} = 8.5 \times 10^{15}\ \mathrm{s}^{-1}$. The difference in pressure of the calibrated valve results in 1.3×10^{19} particles which gives an averaged particle flux of $\Gamma_{\mathrm{H}_2} = 2.6 \times 10^{19}\ \mathrm{s}^{-1}$. Thus, a photon efficiency of 3100 is observed. The error bar in the analysis of the radiation is estimated to be 30% and the pulse average results in maximum of 50% underestimation of the photon efficiency. Langmuir probes in the divertor tiles with a *s*-co-ordinate close to the line of sight, give an electron density of $10^{19}\ \mathrm{m}^{-3}$, with an uncertainty of a factor of two, and an electron temperature of 10–20 eV, which can be taken as an upper limit. The usage of the molecular radiation for T_e-diagnostics [15] indicates electron temperatures above 7 eV. Thus, the photon efficiency of 3100 corresponds to $n_e = 10^{19}\ \mathrm{m}^{-3}$ and $T_e = 10$ eV with error bars as discussed above. Calculations with the collisional radiative model give a photon efficiency of 3200 and 340, with and without extensions, respectively. As can be seen from Figs. 1 and 2, a variation in T_e from 5 to 25 eV and in n_e by a factor of two results in an uncertainty of factor of two for the photon efficiency. Nevertheless, it is obvious that the measurements confirm clearly the results of the extended collisional radiative model within the discussed uncertainties. Similar experiments at TEXTOR [16] give a photon efficiency of 980 at 50 eV and $5 \times 10^{17}\ \mathrm{m}^{-3}$, which is in agreement within the error bars with calculations with and without extensions. At this low electron densities and high electron temperatures the model is less sensitive on the extensions. Systematic measurements of the effective emission rate coefficient XB in microwave discharges with well defined plasma parameters confirm the extended collisional radiative model [10] in the parameter range $n_e = 7 \times 10^{16}$–$5 \times 10^{17}\ \mathrm{m}^{-3}$ and $T_e = 2$–3 eV (see Section 2.1). Furthermore, the influence of quenching, which is important in these experiments ($n_{\mathrm{H}_2} = 10^{20}$–$10^{22}\ \mathrm{m}^{-3}$) is proved.

In summary, the underlying experimental investigations confirm the extended collisional radiative model and demonstrate the importance of dissociative attachment, charge exchange and quenching of excited states in such plasmas. Thus, the photon efficiency necessary for the determination of molecular influxes is experimentally proved. Since high photon efficiencies correspond to weak molecular intensities, the resulting molecular influxes can be comparable to atomic fluxes and may have been underestimated in former experiments or plasma edge codes.

References

[1] P.C. Stangeby, The Plasma Boundary of Magnetic Fusion Devices, Institute of Physics, Bristol, 2000.
[2] Ph. Mertens et al., Plasma Phys. Control. Fusion 43 (2001) 1.
[3] U. Fantz, D. Reiter, B. Heger, D. Coster, J. Nucl. Mater. 290–293 (2001) 367.
[4] K. Behringer, J. Nucl. Mater. 145–147 (1987) 145.
[5] L.C. Johnson, E. Hinnov, J. Quant. Spectrosc. Radiat. Transf. 13 (1973) 333.
[6] K. Sawada, K. Eriguchi, T. Fujimoto, J. Appl. Phys. 73 (1993) 8122.
[7] K. Sawada, T. Fujimoto, J. Appl. Phys. 78 (1995) 2913.
[8] D. Wünderlich, U. Fantz, Max-Planck-Institut für Plasmaphysik, Report, IPP 10/18, 2001.
[9] M.L. Burshtein et al., Opt. Spectrosc. 68 (1990) 166.
[10] B. Heger, PhD thesis, University of Augsburg, 2002.
[11] A.B. Wedding, A.V. Phelps, J. Chem. Phys. 89 (1988) 2965.
[12] R. Janev, private communication.
[13] J.R. Hiskes, Appl. Phys. Lett. 69 (1996) 755.
[14] P.G. Datskos, L.A. Pinnaduwage, J.F. Kielkopf, Phys. Rev. A 55 (1997) 4131.
[15] U. Fantz, B. Heger, D. Wünderlich, Plasma Phys. Control. Fusion 43 (2001) 907.
[16] S. Brezinsek, Report, Jül-3962, 2002.